INVESTIGATION OF LASER DYNAMICS, MODULATION AND CONTROL BY MEANS OF INTRA-CAVITY TIME VARYING PERTURBATION

under the direction of

S. E. Harris

Semi-Annual Status Report No. 6

for

NASA Grant NGR-05-020-103

National Aeronautics and Space Administration

Washington, D. C.

for the period

1 August 1968 – 31 January 1969

M. L. Report No. 1724

February 1969

Microwave Laboratory
W. W. Hansen Laboratories of Physics
Stanford University
Stanford, California

STAFF

NASA Grant NGR-05-020-103

for the period

1 August 1968 – 31 January 1969

PRINCIPAL INVESTIGATOR

S. E. Harris

PROFESSOR

A. E. Siegman

RESEARCH ASSISTANTS

R. L. Byer

J. F. Young

T. K. S. Nieh

INTRODUCTION

The work under this grant is generally concerned with the generation, control, and stabilization of optical frequency radiation. In particular, we are concerned with obtaining tunable optical sources by means of non-linear optical techniques. During this period we have proposed and begun work on a new type of electronically tunable optical filter. The basic idea is to make use of acousto-optic diffraction in an anisotropic optical media. We expect that bandwidths a few angstroms wide which are completely tunable over the visible spectrum may be attained.

Work on other projects is continued as described in the following sections.

During this period the following publication has been submitted for publication and is included as an Appendix:

S. E. Harris and R. W. Wallace, "Proposed Acousto-Optic Tunable Filter," to be published in the J. Opt. Soc. Am.

1. Parametric Oscillation at Optical Frequencies (J. F. Young, S. E. Harris)

The cw parametric oscillator described in the Semi-Annual Status Report No. 5 demonstrated the general validity of parametric theory and the feasibility of such tunable optical oscillators. The ultimate utility of these sources will be determined by their stability and bandwidth and during the past six months we have been primarily concerned with techniques to realize greater stability of parametric oscillators.

The basic parametric gain bandwidth is $1/bL$,[1] where L is the crystal length and b is a constant depending on dispersion. Typically this represents several wavenumbers and includes a large number of longitudinal oscillator cavity modes. Competition between these modes and the energy criteria $\nu_s + \nu_i = \nu_p$ determines the characteristics of the oscillator. In our previous oscillator both signal and idler waves were resonant and we adjusted the cavity length so that the idler intermode spacing was identical to that of the pump, while, because of crystal dispersion, the signal modes had a smaller spacing. As shown in Fig. 1 a set of pump modes and a set of resonant idler modes interact to drive a single signal mode. Thus one output wave of the oscillator is forced to have a narrow bandwidth. However, if the pump frequency shifts by a small amount the signal and idler waves in the oscillator cavity no longer satisfy the energy criteria and oscillation commences at a new set of signal and idler frequencies. We believe that this was the source of the pulsating output of our oscillator and the observed jumping of the single signal mode within the gain bandwidth.

---

[1] R. L. Byer and S. E. Harris, "Power and Bandwidth of Spontaneous Parametric Emission," Phys. Rev. 168, 3, 1064-1068 (15 April 1968).

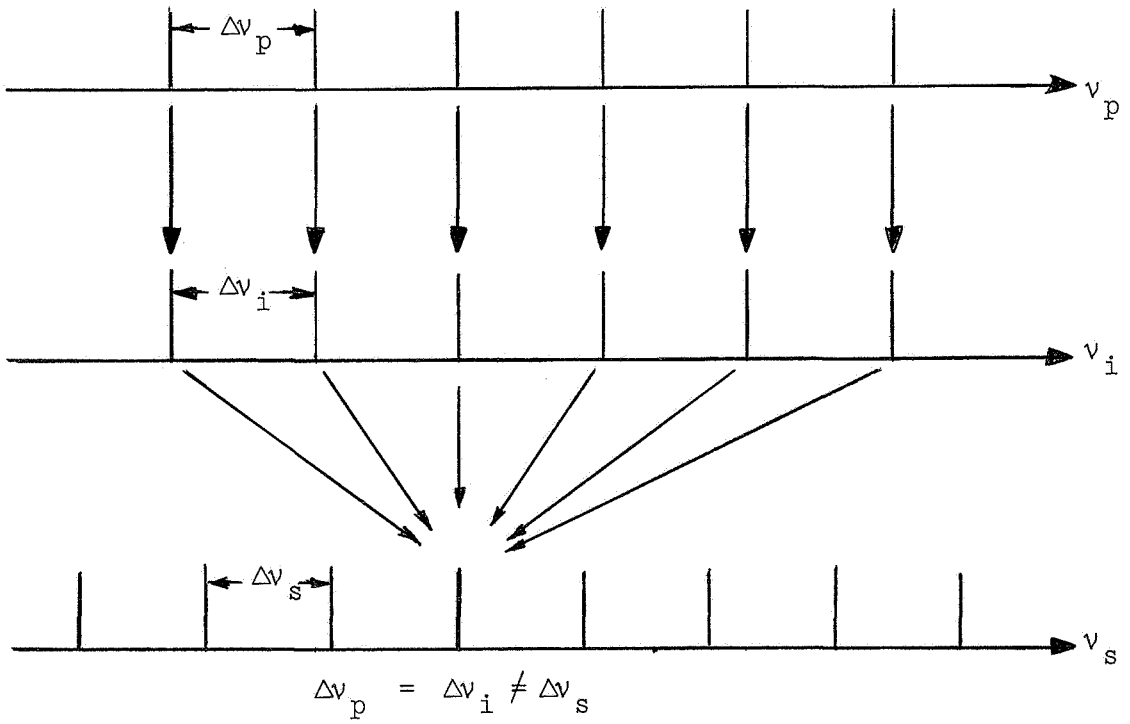

FIG. 1--Interaction of a comb of pump and idler modes to drive a single signal mode.

An oscillator which resonates only a single parametric wave will not exhibit this instability since the free wave may be generated at any frequencies necessary to satisfy the energy criteria. Therefore the resonating wave should remain constant in frequency even if the pump frequency or intermode interval shifts, as long as the oscillator cavity length is constant. This increased stability is gained at the expense of a considerably larger threshold. At present, unfortunately, we do not have a cw pump source with an output power capable of achieving these threshold gains. We therefore proposed to build the oscillator by placing the nonlinear crystal inside the laser resonator to make use of the larger circulating powers. Typical crystal absorption loss seen by the laser can be compensated for by replacing the 4% transmitting output mirror with an opaque mirror, and the circulating power should remain high, about 30 watts. The threshold pump power for the singly resonant oscillator of Fig. 2 is 6 watts, based on estimated losses of 2% and a 5 mm crystal of $Ba_2NaNb_5O_{15}$. The internal oscillator should be well above threshold.

The argon laser bench and mirror mounts were redesigned and rebuilt to provide greater stability and to permit insertion of the various optical components within the laser resonator. A simple lens was used in place of the beam splitter for the initial pump power measurements. The cavity was assembled without a crystal and the laser circulating power was 18 watts at 514.5 nm. This reduction was due to increased absorption and cavity losses and a reduced coupling between the cavity modes and the argon plasma volume. The latter factor had been minimized by designing the optics using a computer program we wrote.

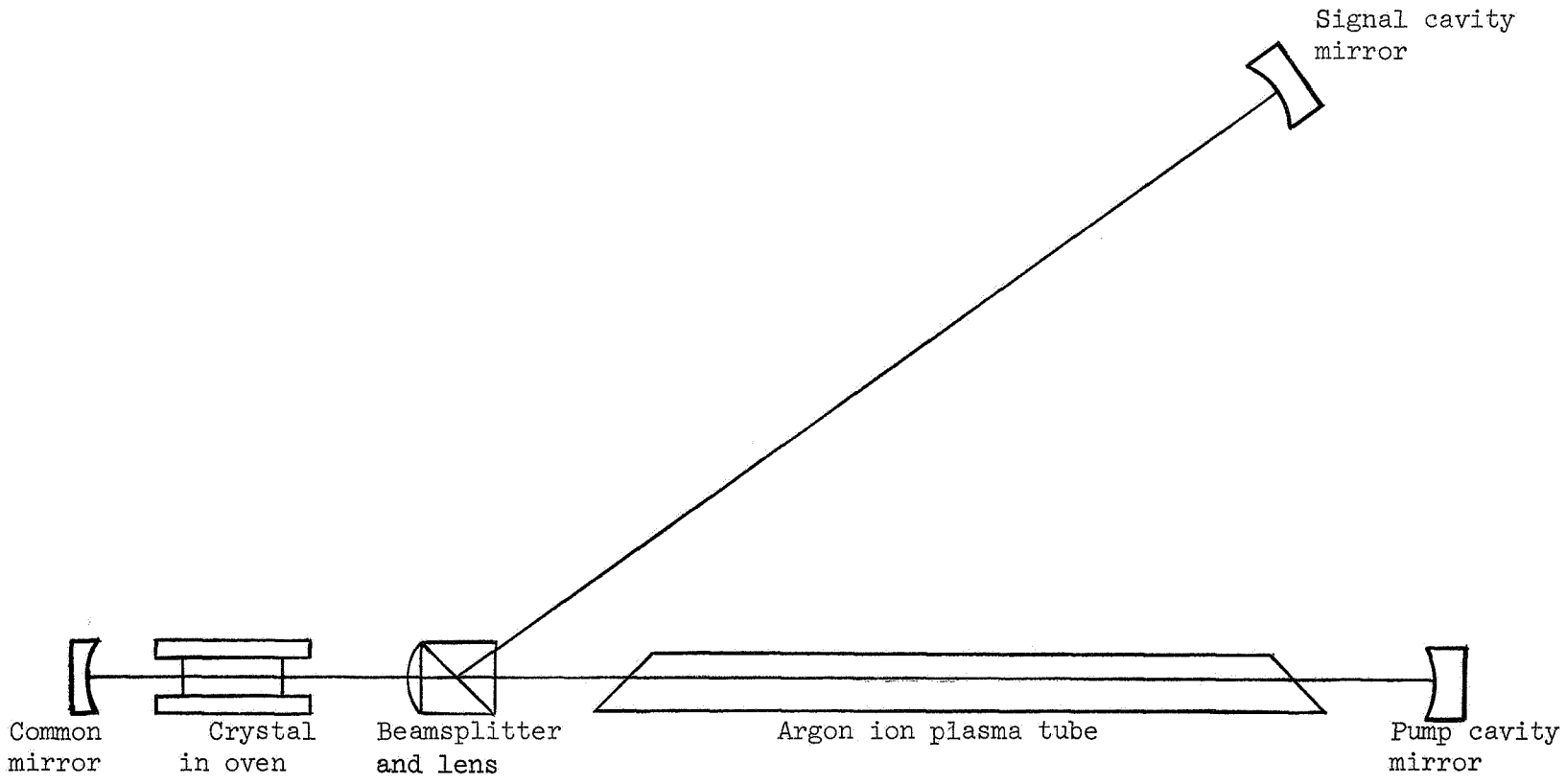

FIG. 2--Internal single resonant parametric oscillator.

Two crystals were prepared for this cavity: an a-axis grown crystal 5 mm long and a c-axis grown crystal 7 mm long. Both crystals contained conspicuous stria which we hoped to get through because of the small spot size within the crystal.

The results with both crystals was unexpectedly poor. A maximum of only 0.8 watts circulating power at 514.5 nm was observed with the a-axis grown crystal. This low power and the observed transverse mode distortions indicate that small angle scattering and/or other loss mechanisms are more important than simple absorption losses in determining laser power. Lowering the average power level with a chopper did not improve the peak powers, but it is possible that some type of fast optical damage is limiting the circulating power. A 16 mm crystal of $LiNbO_3$ was also placed in the cavity to determine if its greater optical quality could compensate for its lower nonlinearity. Power levels were not significantly higher.

On the basis of these results we have postponed further work on this experiment until better quality $Ba_2NaNb_5O_{15}$ crystals are available. We continue to work closely with the Materials Research Center at Stanford and we feel confident that progress will be made. This experiment indicated clearly that a-axis grown crystals are superior to c-axis grown, and we are concentrating our efforts on a-axis boules.

We are currently in the initial phases of a new experiment. It appears possible to use the peak power of a phase-locked argon laser to overcome threshold of a single resonant oscillator. This avoids placing a crystal within the laser cavity. The phase-locked oscillator output, while not true cw, should be quite useful in studying atomic

lifetimes, possibly in communcation, and in providing a means to accurately stabilize the oscillator cavity length. It should be possible to gain a factor of 10 or more in effective pump power using a quartz acoustic loss modulation element for phase-locking. Our initial goal is to build the modulator and to determine the available pump power.

2. Visible CW Parametric Oscillator (R. L. Byer)

The experimental results reported in the last report have been more fully analyzed and compared with theoretical predictions. In this report a discussion of the theory of the parametric oscillator is given along with comparison of theory and experiment. The results appear in a complete form in the thesis of R. L. Byer.

The theory for the resonant signal and idler parametric oscillator was studied and the following important results were obtained. The threshold condition was derived for a Gaussian beam in the near field approximation and was found to be

$$P_p(\text{threshold}) = \frac{\pi a_s a_i \epsilon_0^3 c^3 n_i n_s n_p}{4\omega_i \omega_s d_{31}^2 L^2 \operatorname{sinc}^2(\Delta kL)} (w_s^2 + w_i^2)$$

where a_i and a_s are the single pass idler and signal loss, n_i, n_s and n_p are the crystal indices of refraction at the idler, signal, and pump, L is the crystal length, d_{31} the nonlinear coefficient, and w_s the beam radii at the signal and idler. For minimum threshold the beam radii are chosen to satisfy the condition

$$\frac{1}{w_p^2} = \frac{1}{w_s^2} + \frac{1}{w_i^2}$$

Using the parameters for the present experiment of $a_i = 1.8\%$, $a_s = 5.4\%$, $n_i n_s n_p = 11.3$ and $w_s = 34$ microns and $w_i = 67$ microns the threshold is calculated to be 460 mW ± 20% . This compares very well with the measured threshold of 410 mW. Figure 3 and Fig. 4 show the cavity loss and cavity mode dimensions for this oscillator. The 300 Å low loss region allowed tuning over this range in a continuous manner by changing the crystal temperature. The rate of tuning limited by the oven thermal mass was 60 Å per minute. In the future broadband mirrors could allow a wider tuning range limited only by the transparency of $LiNbO_3$ in the blue and IR regions of the spectrum.

The solution of the steady-state equations led to the expressions governing the oscillator's output power and reflected pump power. Figure 5 shows a plot of

$$\frac{a_s/a_{cs}\ P_{signal}(OUT)}{\omega_s/\omega_p\ \ P_{pump}(INPUT)} = \left[\left(\frac{P_p(input)}{P_p(threshold)}\right)^{1/2} - 1\right]$$

and

$$\frac{P_p(reflected)}{P_p(input)} = \left[\left(\frac{P_p(input)}{P_p(threshold)}\right)^{1/2} - 1\right]^2 .$$

The figure shows that the maximum oscillator efficiency of 25% is obtained at four times above threshold. The efficiency is limited due to the generation of a reflected pump wave caused by mixing of the signal and idler beams in the crystal traveling in the back direction without the pump wave present.

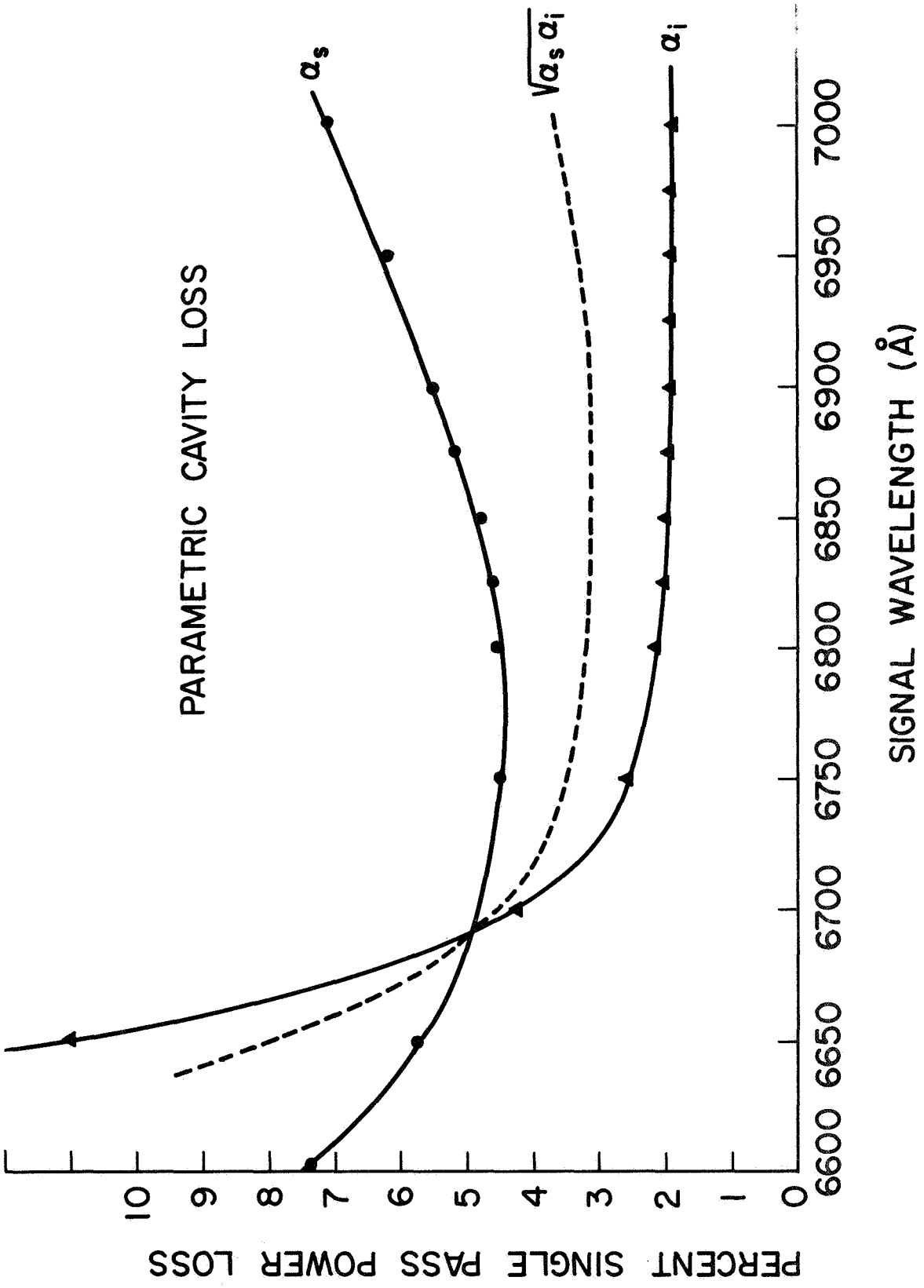

FIG. 3--Absorption in $LiNbO_3$ in the visible region.

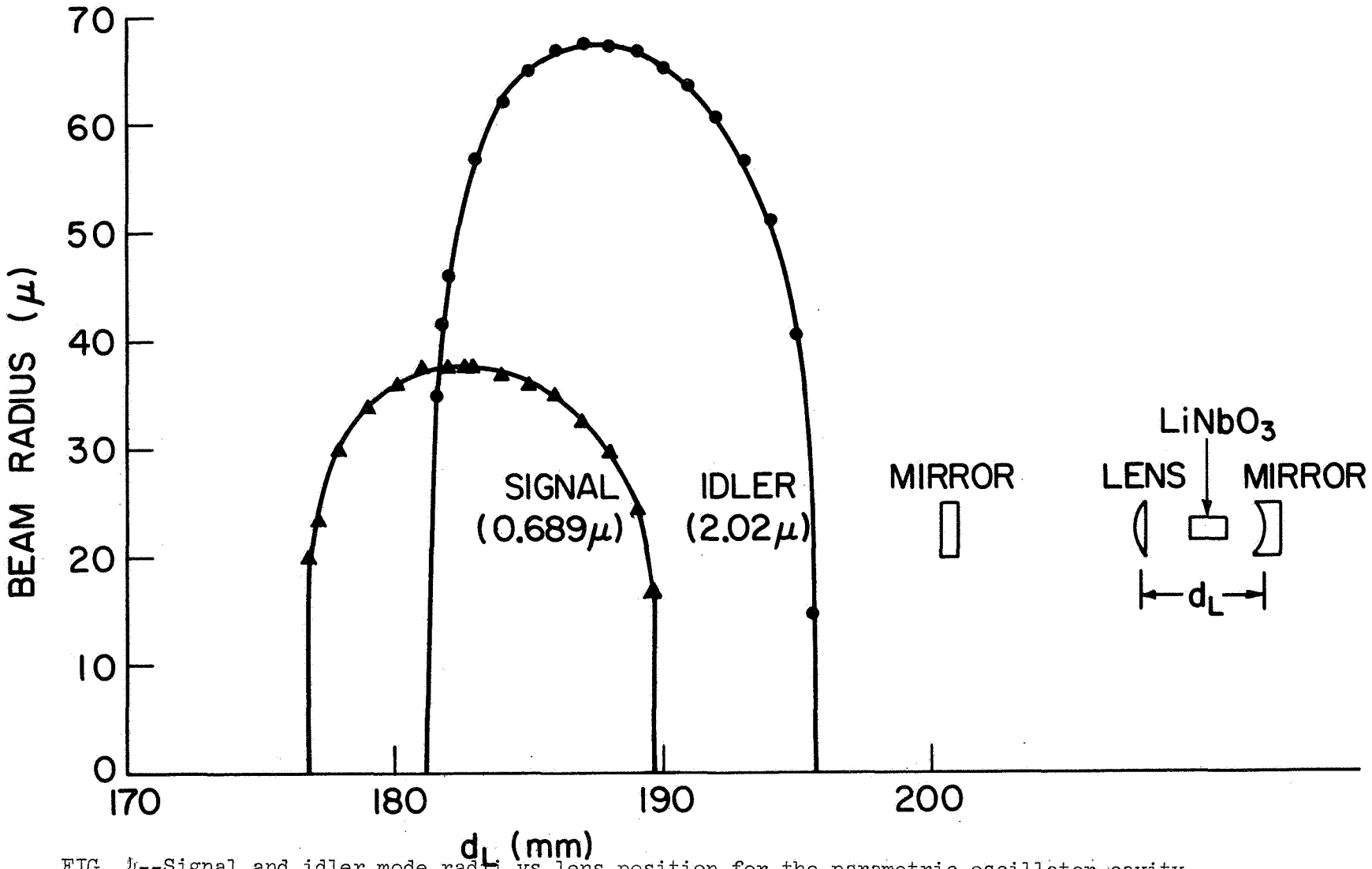

FIG. 4--Signal and idler mode radii vs lens position for the parametric oscillator cavity.

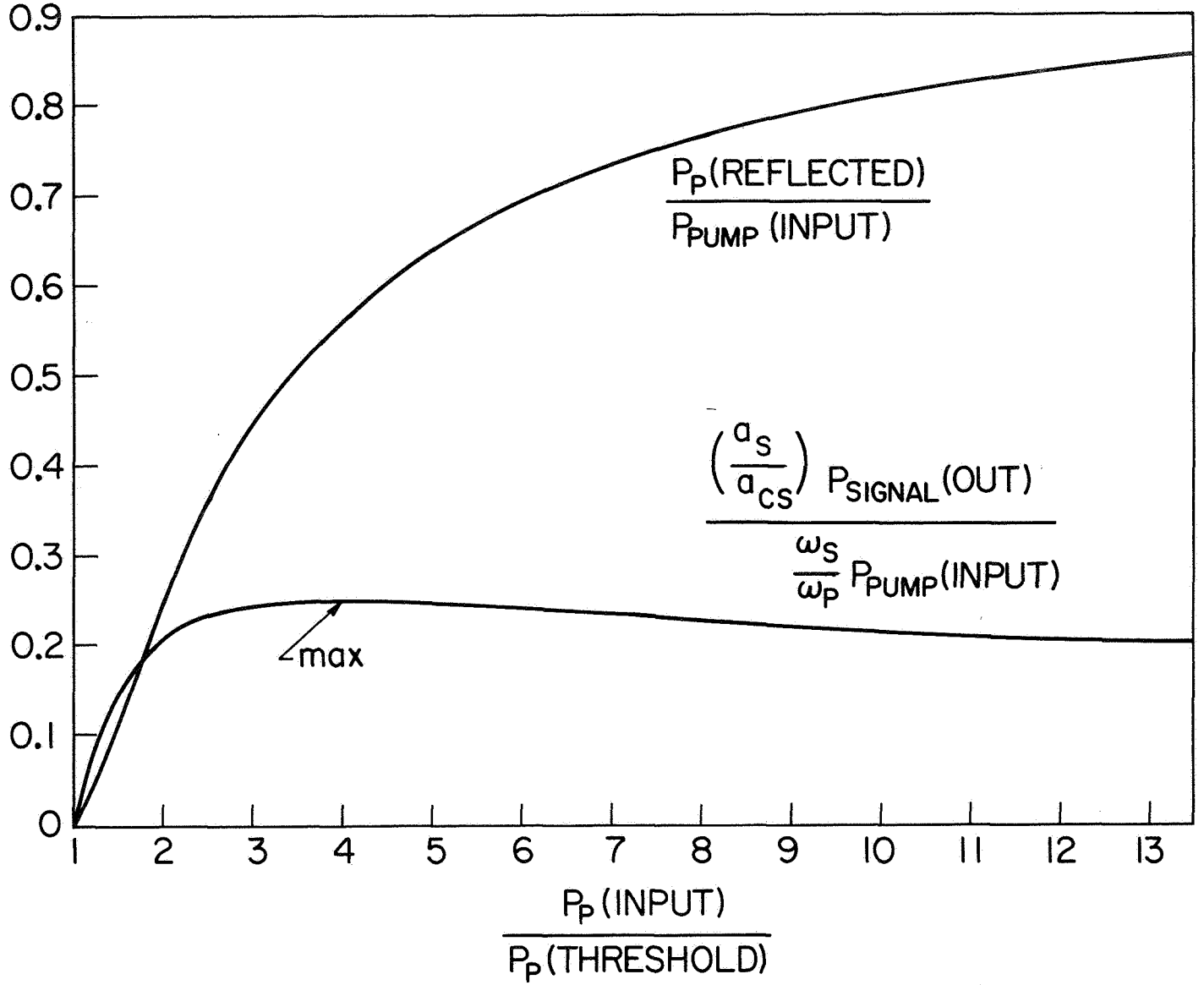

FIG. 5--Efficiency of the external oscillator as a function of $P_p(\text{input})/P_p$ (threshold).

If the reflected pump wave is eliminated the power that is in the reflected pump wave appears in the signal and idler waves. The generated signal power then becomes

$$\frac{(a_s/a_{cs})\ P_s(\text{out})}{(\omega_s/\omega_p)\ P_p(\text{threshold})} = \frac{1}{2}\left[\frac{P_0(\text{input})}{P_p(\text{threshold})} - 1\right]$$

and the idler power is

$$\frac{(a_i/a_{ci})P_i(\text{out})}{(\omega_i/\omega_p)\ P_p(\text{threshold})} = \frac{1}{2}\left[\frac{P_p(\text{input})}{P_p(\text{threshold})} - 1\right]$$

In this case the parametric oscillator's efficiency can approach 100% as the amount above threshold increases. Methods of eliminating the back reflected pump wave include quarter wave plates, ring cavities and off-axis confocal cavities. No attempt was made in this experiment to eliminate the back reflected pump wave.

The theory also predicts a value of mirror transmission that gives the optimum output coupling for the oscillator. If we let γ be the ratio of the coupling loss to the dissipative loss at the signal, i.e.,

$$\gamma = \frac{a_{cs}}{a_{ds}}$$

and let N be the number of times the oscillator is above threshold for no coupling loss at the signal, then the optimum coupling condition is found for a γ satisfying the equation

$$\gamma^3 + (3-N/4)\ \gamma^2 + (3-N)\ \gamma + (1-N) = 0$$

The solution of this cubic equation is plotted in Fig. 6.

The rise time of the oscillator was also derived and was found to be

$$t_{rt} = \frac{(L_c/c)\ \ln [P_s/P_s(0)]}{2a\ [\sqrt{n}-1]}$$

where L_c is the cavity length, P_s is the steady-state signal power, $P_s(0)$ is the noise signal power, a is the signal pass loss, and n is the number of times the oscillator is above threshold.

For the present case $L_c = 135$ cm , $a = 3.0\%$, and $n = 2$ we find that

$$t_{rt} = 4.0\ \mu\text{sec}$$

The experimentally measured rise time was approximately 6.0 μsec which is in good agreement considering that the value of n was estimated and that the oscillator was assumed to be turned on rapidly compared to the rise time.

The output power of the oscillator was quasi cw with random pulse variations of 1 msec to less that 0.1 msec in duration. Figure 7 is an oscilloscope trace of the output power at the signal. The peak to average power ratio was about 5.0 ± 0.05 . At 2.8 times above threshold this gave an experimental peak power output of 14.4 mW.

From the theory, with the ratio of signal loss to output coupling that was observed experimentally, we calculate that the oscillator's output power should be 14.0 mW at 2.8 times above threshold. The agreement is a good verification of theory and leads one to believe that in the future efficient cw parametric oscillators will be constructed.

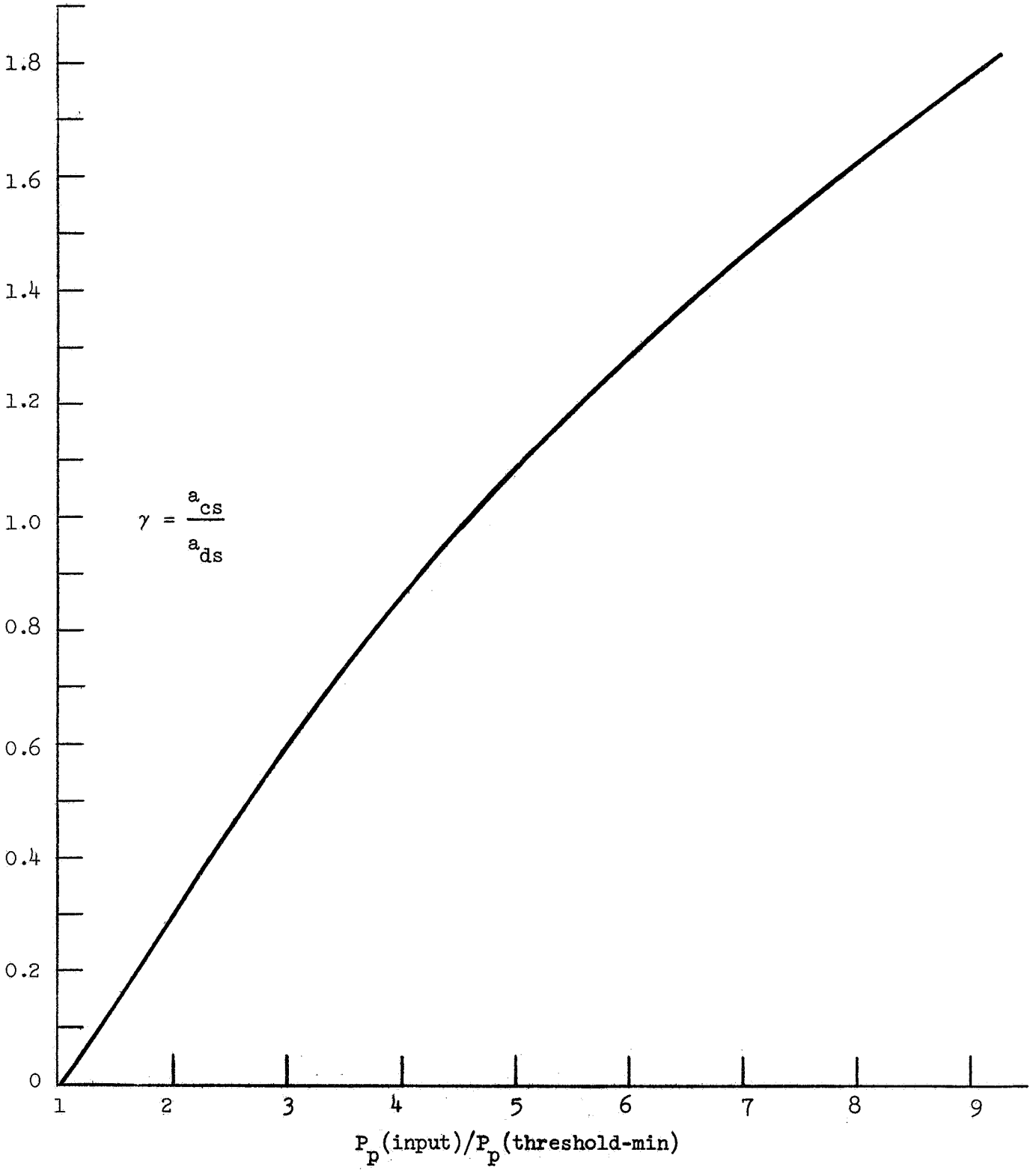

FIG. 6--Optimum output coupling for the external oscillator vs P_p(input)/P_p(threshold-min).

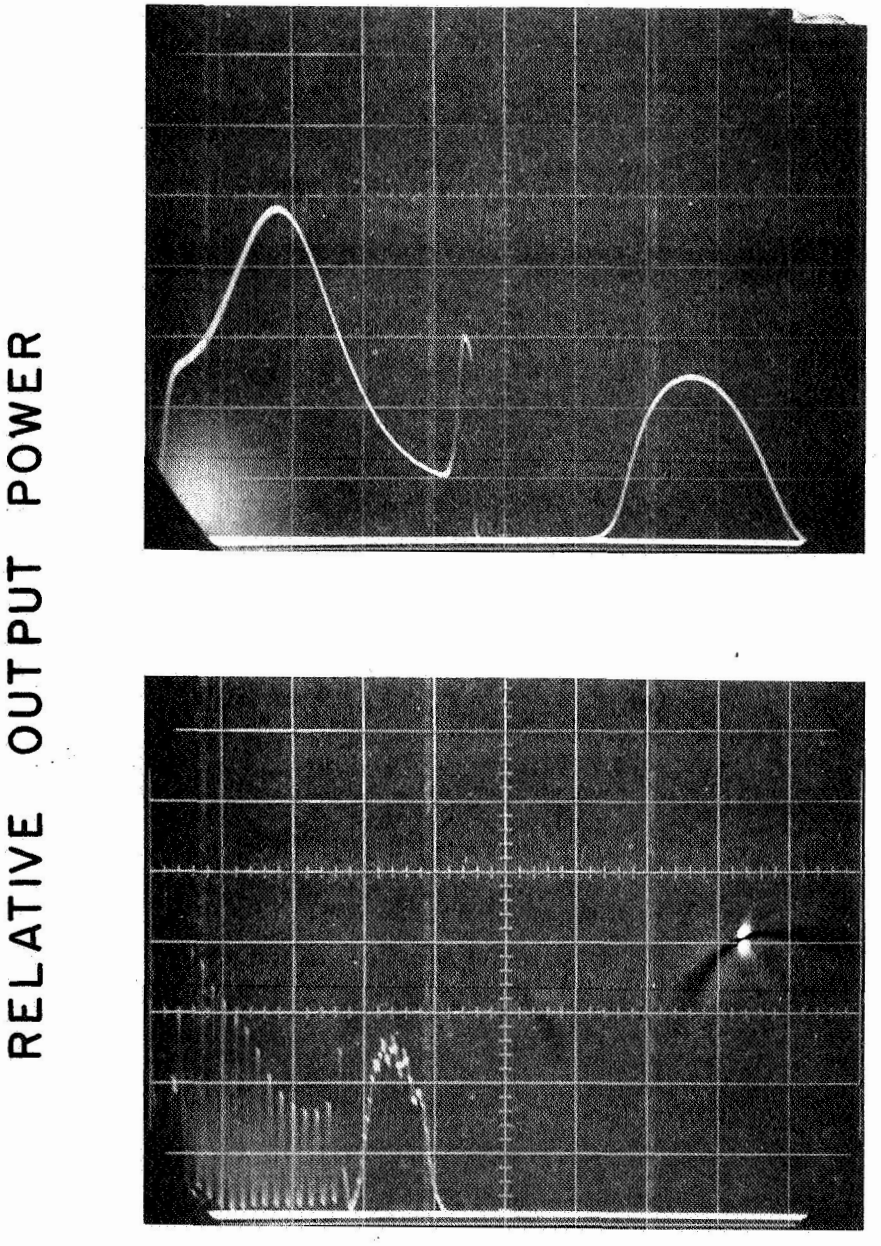

FIG. 7--Signal output power vs time at a 0.1 msec/cm scale.

This is the first parametric oscillator to be pumped with the average power of the multi-longitudinal mode laser. To achieve this pump condition the length of the parametric oscillator's cavity had to be set equal to the pump laser cavity length. Figure 8 shows the parametric oscillator's power as its cavity length was scanned through the proper length. This clearly illustrates that the average pump power was indeed effective in driving the parametric oscillator.

This oscillator even though operating about two times above threshold did run for more than a two month period. Figures 9, 10, and 11 are photographs of the main oscillator components and serve to illustrate that the device is relatively uncomplicated in its final form on the bench.

Since the oscillator was operating more than two times above threshold a phase locking crystal could be inserted into the pump laser cavity and still leave enough power at 5145 Å to remain above threshold. This experiment was attempted and the pump laser was phase locked to drive the oscillator with the peak power of the phase locked pulses. The results are shown in Fig. 12. It is seen that the oscillator did not run during the phase locking time. This negative result was checked for artifact and none was found. The unexpected result is now a subject of further investigation. Also suggested for study are methods of lowering the threshold of the oscillator, improving its bandwidth and its stability and increasing its tuning rate and range.

The first cw visible parametric oscillator demonstrated that the theory is correct in all aspects and that the oscillators are indeed realizable. The next step is to improve on these results leading toward a more useful and practical source of coherent tunable radiation.

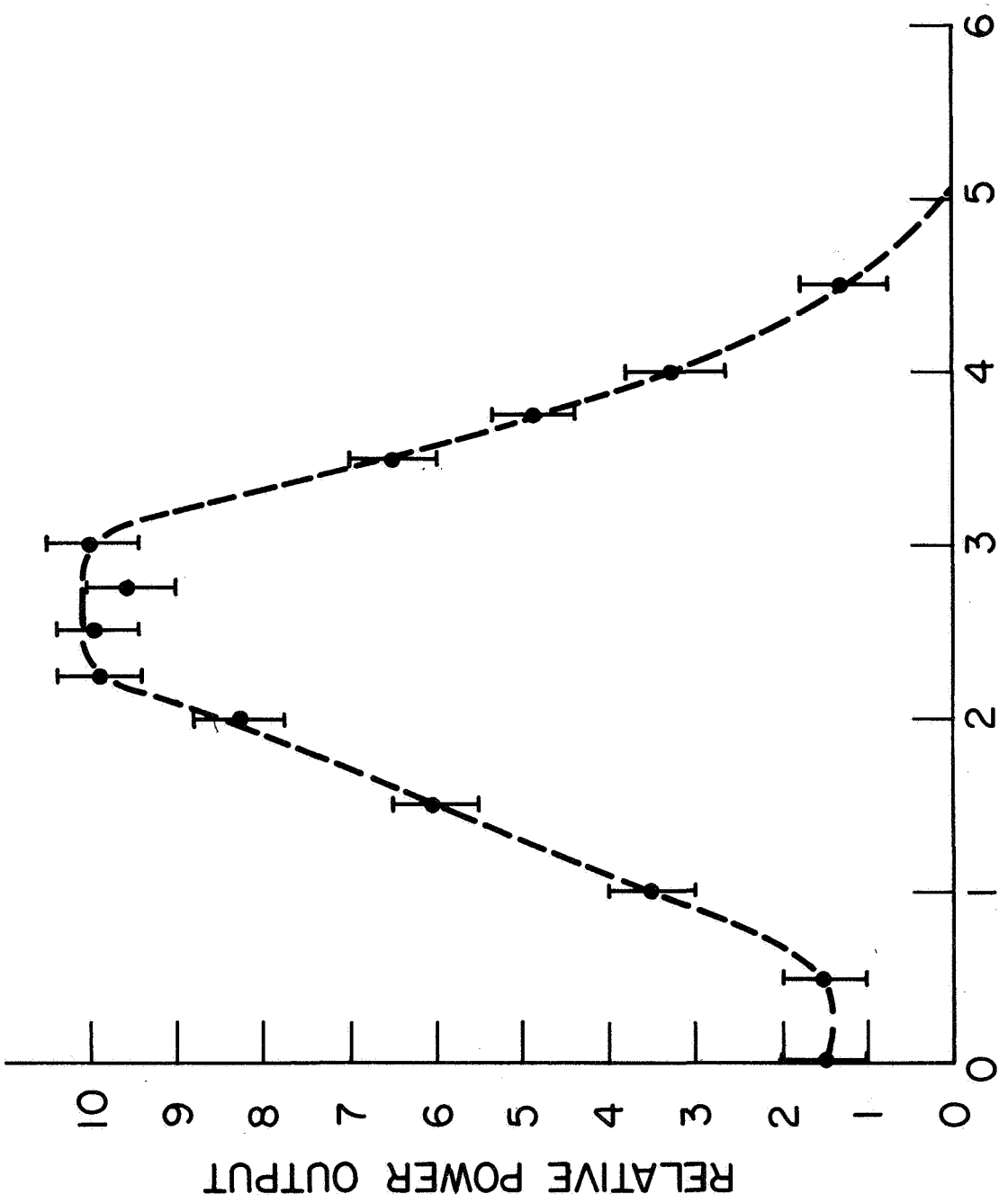

FIG. 8--Signal output power vs the c/2L length of the parametric cavity.

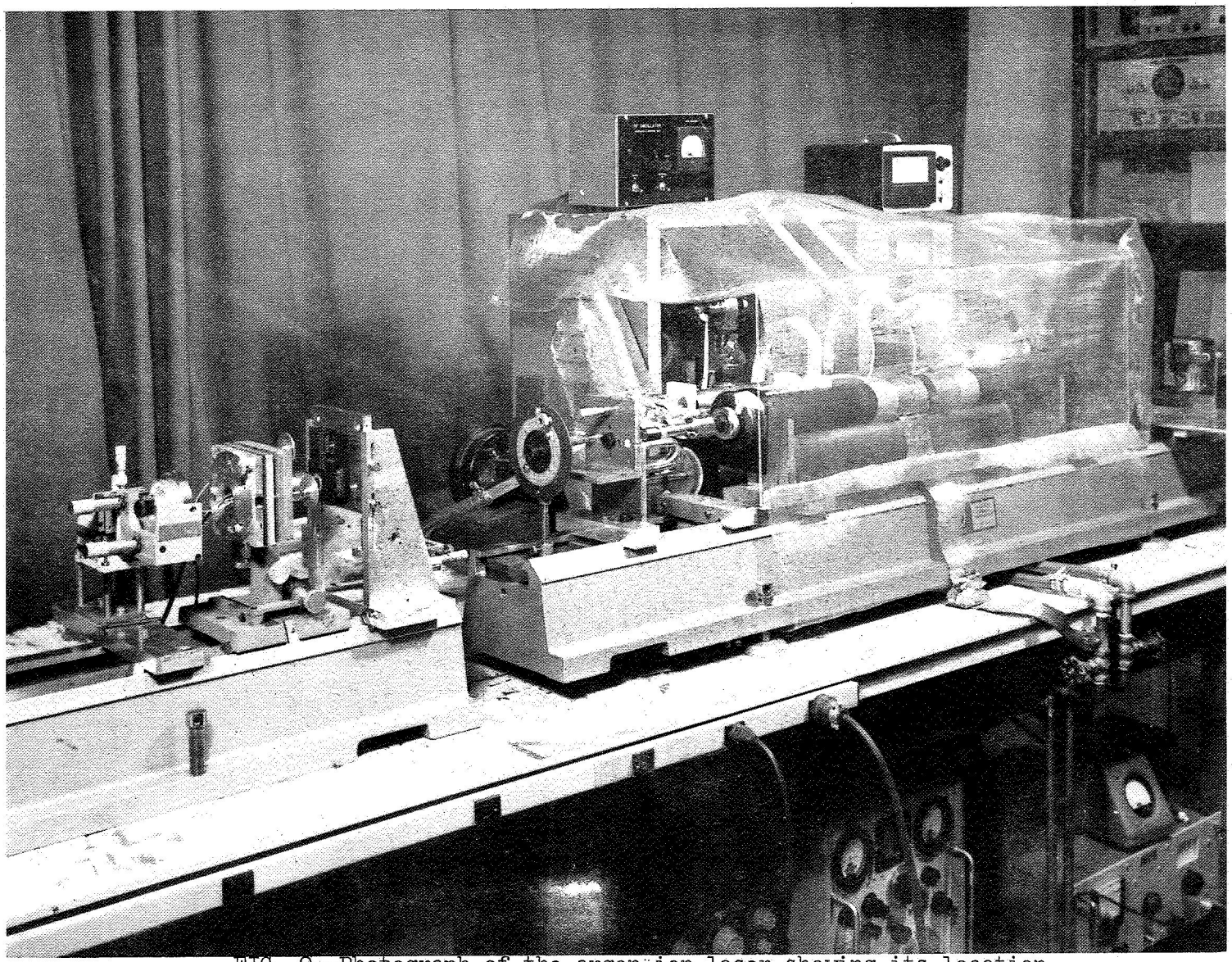

FIG. 9--Photograph of the argon ion laser showing its location with respect to the parametric oscillator cavity.

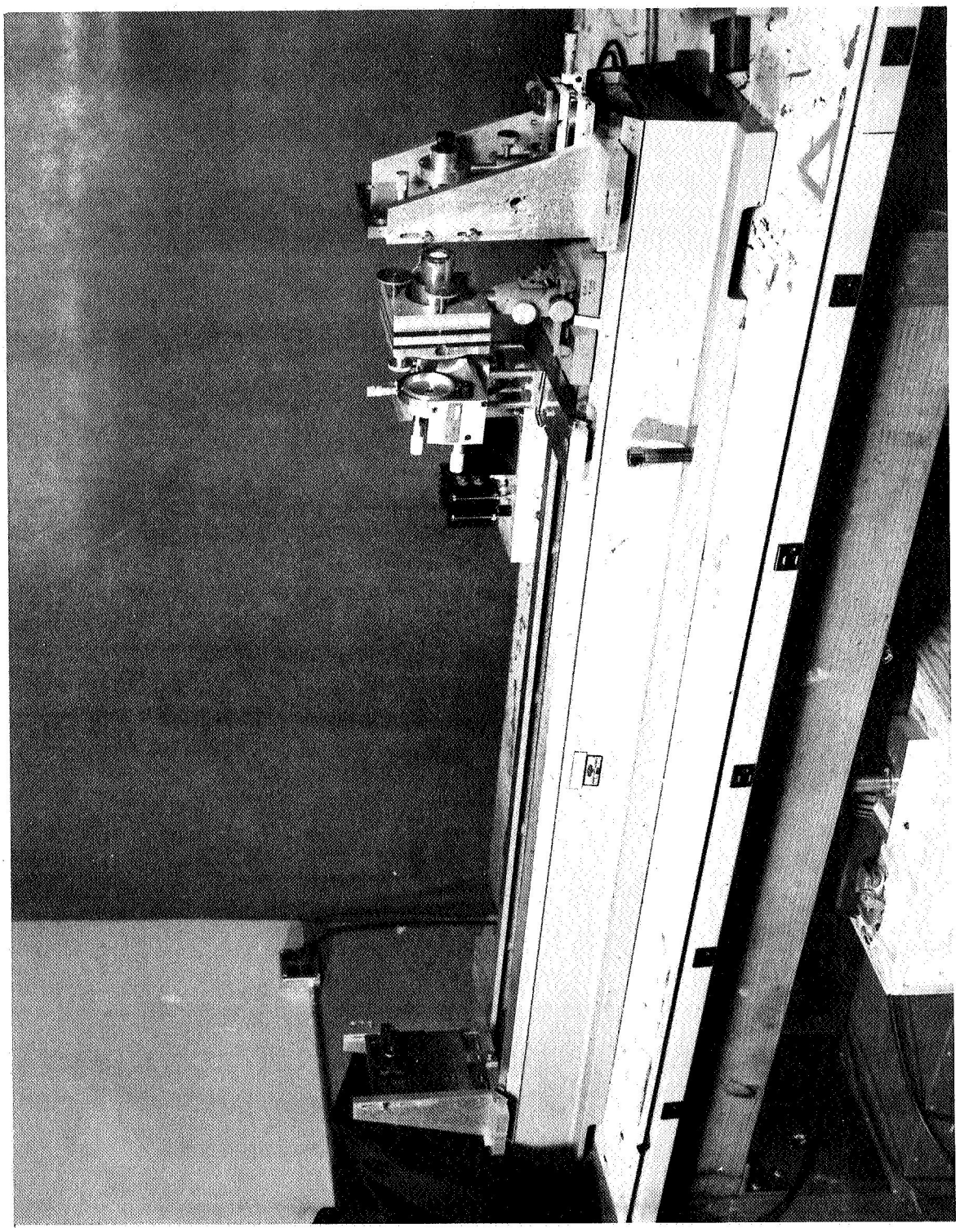

FIG.10--Photograph of the parametric oscillator cavity.

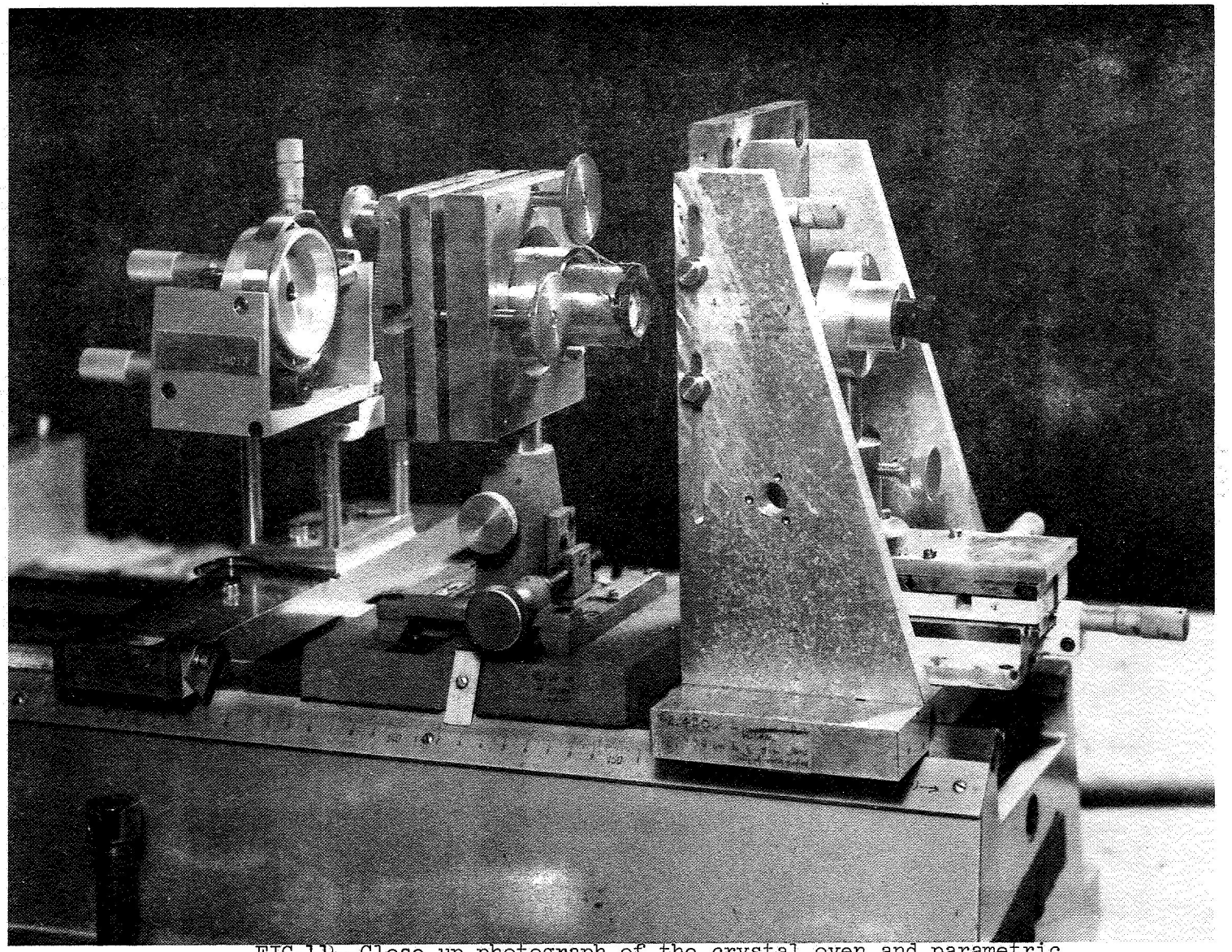

FIG.11--Close up photograph of the crystal oven and parametric oscillator cavity elements.

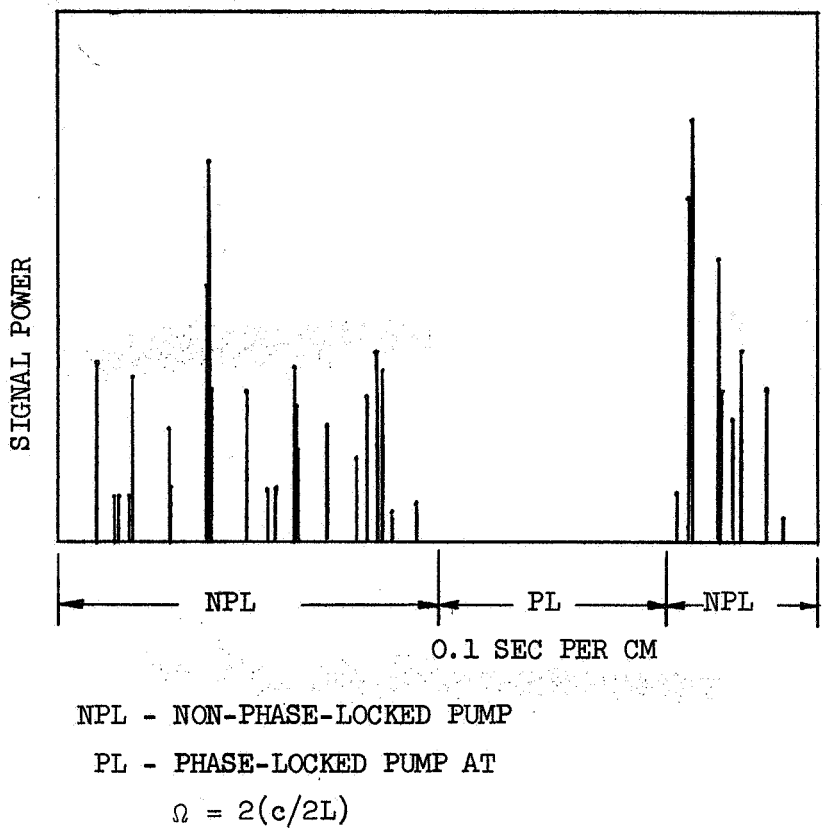

FIG. 12--Oscilloscope trace of preliminary phase locking results.

3. Acousto-Optic Tunable Filter (S. E. Harris and S. Nieh)

We report a proposed acousto-optic tunable filter. We summarize the basic principle utilized in this proposed device and will give one specific example. A complete detail of this proposed device is in the paper "Proposed Acousto-Optic Tunable Filter," by S. E. Harris and R. W. Wallace which is included in this report as an Appendix.

The principle utilized is collinear acousto-optic diffraction in an optically anisotropic medium. The band of optical frequencies passed is selected by the driving acoustic frequency. We chose an orientation such that the effective photoelastic constant is largest. With a suitably chosen acoustic beam, an incident optical signal of one polarization is cumulatively diffracted into the orthogonal polarization. For a given acoustic frequency only a small range of optical frequencies satisfy the phase matching condition for this collinear diffraction in anisotropic media. Tuning of the passband of the filter is then accomplished by changing the acoustic frequency.

We shall discuss a specific example using $LiNbO_3$. The filter consists of an input polarizer, a crystal with an acoustic transducer and an output polarizer. The acoustic beam and the optical beam travel collinearly along the y axis of the crystal along which the acousto-optic interaction takes place.

The input beam is an extraordinary wave polarized along a z axis. The output or diffracted optical beam will be an ordinary wave polarized along an x axis. The acoustic shear wave supplies the missing k vector to satisfy the momentum matching condition.

The interaction between the acoustic and optical waves is due to photoelastic effect. The creation of a driving polarization is the result of this photoelastic effect.

$$\hat{P}_x = - e_0 n_0^2 n_e^2 P_{41} \hat{S}_6 \hat{E}_z$$

$$\hat{P}_z = - e_0 n_0^2 n_e^2 P_{41} \hat{S}_6 \hat{E}_x$$

where

e_0	dielectric constant of free space
n_0	refractive index for ordinary wave
n_e	refractive index for extraordinary wave
P_{41}	photo-elastic constant responsible for interaction
$\hat{S}_6$	acoustic shear wave amplitude
$\hat{E}_x$	E field in x direction
$\hat{E}_z$	E field in z direction.

Next we introduce the one dimensional driven wave equation for lossless media

$$\frac{\partial^2 \hat{E}}{\partial y^2} - \frac{1}{c^2} \frac{\partial^2 \hat{E}}{\partial t^2} = \mu_0 \frac{\partial^2 \hat{P}}{\partial t^2}$$

Approximating that $E_x(y)$ and $E_z(y)$ are quasi-dc, we obtain the coupled equations of motion for E_x and E_z (assuming the acoustic wave propagate losslessly in the crystal)

$$\frac{dE_x}{dy} = j \frac{n_0 n_e^2 P_{41} \omega_0}{4c} S_6 E_z \exp j\Delta ky$$

$$\frac{dE_z}{dy} = j \frac{n_e n_0^2 P_{41} \omega_e}{4c} S_6^* E_x \exp -j\Delta ky$$

where $\Delta k = k_0 - k_e - k_a$ is the vector mismatch

ω_e optical frequency of extraordinary wave

ω_0 optical frequency of ordinary wave.

Now we solve the coupled equations subject to the boundary condition $E_x = 0$ and $E_z = E_z(0)$ and $y = 0$. We find for zero momentum mismatch,

$$\frac{P_x(L)}{P_z(0)} = \sin^2 \Gamma L$$

where

$$\Gamma^2 = \frac{n_0^3 n_e^3 P_{41}^2 \omega_0 \omega_e}{16c^2} |S_6|^2$$

$P_x(L)$ output power at $y = L$

$P_z(0)$ input power at $y = 0$.

We see that theoretically 100% transmission is achieved when $\Gamma L = \pi/2$. For a five cm long $LiNbO_3$ at optical frequency of $\lambda_0 = 5000$ Å , we find for 100% transmission a power density of 14 mW per mm^2 of filter aperture is required.

The frequency response of the filter is determined by the variation of Δk as optical frequency is changed. We can write the optical frequency response function of the filter as

$$H(f) = \pi^2 \frac{\sin^2 \frac{1}{2}(\pi^2 + b^2 L^2 \Delta y^2)^{1/2}}{\pi^2 + b^2 L^2 \Delta y^2}$$

where Δy is change in wavenumber of the optical frequency

and $b = \frac{\Delta k}{\Delta y}$.

In this example at 5000 Å the total half-power bandwidth is $1.25\ cm^{-1} = .31$ Å .

The filter is tuned by changing acoustic frequency which changes the magnitude of its k vector. The acoustic frequency that will pass optical frequency at λ_0 is

$$f_a = \frac{V}{\lambda_0}(n_0 - n_e)$$

V is acoustic velocity 4×10^5 cm/sec

$n_0 = 2.3$, $n_e = 2.2$

Acoustic frequency	Optical wavelength
428 mc/s	4000 Å
680 mc/s	5000 Å
990 mc/s	7000 Å

Rate of change of optical wavenumber per cycle change in the acoustic frequency is $\Delta y/\Delta f_a = 2\pi/bV$. In this example the average tuning rate is about 20 wavenumbers per Mc/s change of acoustic frequency.

Optical angular aperture is due to $\bar{k}$ vector mismatch. For nearly collinear propagation we obtain

$$\Delta k \cong \frac{\pi}{\lambda}\Delta n \psi^2$$

where

$\psi = \sqrt{\frac{\lambda}{L\Delta n}}$ is the half-angle aperture inside the crystal.

We expect the most difficulty to come from acoustic transducers. At present we are limited by their power handling capability, bandwidth, and conversion efficiency. Also it is not easy to obtain a sample of $LiNbO_3$ 5 cm long and of good optical quality.

There are a number of other crystals which are currently under consideration e.g., αHlO_3 , quartz and sapphire. The construction of an experimental model of an acousto-optic filter will begin shortly in our laboratory.

APPENDIX 1

PROPOSED ACOUSTO-OPTIC TUNABLE FILTER

by

S. E. Harris and R. W. Wallace

Microwave Laboratory Report No. 1680

September 1968

PROPOSED ACOUSTO-OPTIC TUNABLE FILTER*

by

S. E. Harris and R. W. Wallace

Department of Electrical Engineering
Stanford University
Stanford, California

ABSTRACT

This paper proposes a new type of electronically tunable optical filter. The basic idea is to utilize collinear acousto-optic diffraction in an optically anisotropic media. By changing the driving acoustic frequency the band of optical frequencies which the filter will pass may be changed. It is shown that a $LiNbO_3$ acousto-optic filter with a pass band approximately 1.3 cm^{-1} wide which is tunable from 4000 Å to 7000 Å by changing the acoustic frequency from 428 Mc to 990 Mc should be obtainable. For this case, the angular aperture will be about 1.5°, and it will be possible to attain 100% (theoretical) transmission at the filter center frequency at an expenditure of about 14 mw of acoustic power per mm^2 of filter aperture.

*The work reported here was sponsored by the National Aeronautics and Space Administration under Grant NGR-05-020-103.

PROPOSED ACOUSTO-OPTIC TUNABLE FILTER

by

S. E. Harris and R. W. Wallace

I. INTRODUCTION

In this paper we propose a new type of electronically tunable optical filter. The basic idea is to utilize collinear acousto-optic diffraction in an optically anisotropic media.[1] A crystal orientation is chosen such that an incident optical signal of one polarization is diffracted into the orthogonal polarization by the acoustic beam. Only a small range of optical frequencies will satisfy momentum matching between the incident optical signal, the acoustic wave, and the orthogonally polarized optical signal; and only this small range of frequencies will be cumulatively diffracted into the orthogonal polarization. By changing the acoustic frequency, the band of optical frequencies which the filter will pass may be changed. It will be shown in the example below that a $LiNbO_3$ acousto-optic filter having a pass band approximately 1.3 cm^{-1} wide which is tunable from 4000 Å to 7000 Å by changing the acoustic frequency from 428 Mc to 990 Mc should be obtainable. For this case, the angular aperture will be about 1.5°, and it will be possible to attain 100% (theoretical) transmission at the filter center frequency at an expenditure of about 14 mw of propagating acoustic power per mm^2 of filter aperture.

II. ANALYSIS

The proposed acousto-optic filter consists of an input polarizer, a crystal with an appropriate acoustic transducer, and an output polarizer. There exist a number of different crystal orientations, involving either longitudinal or shear waves which allow collinear diffraction of light into the orthogonal polarization. One possible configuration for the filter using $LiNbO_3$ is shown in Fig. 1. In this case the acoustic wave is brought in as a longitudinal wave which is then converted to a shear wave upon reflection at the input face of the crystal.[2] The acoustic shear wave and the input optical beam then propagate collinearly down the y-axis of the crystal, along which the acousto-optic interaction takes place.

We take the input optical beam to be an extraordinary wave polarized along the z or optic axis of the crystal. The output or diffracted optical beam will be an ordinary wave polarized along the x-axis of the crystal. The acoustic wave which is necessary to accomplish the diffraction into the orthogonal polarization is an S_6 shear wave, and is set up in the configuration of Fig. 1. The three waves are taken as plane waves and are given by

$$\begin{aligned}
\hat{E}_z(y,t) &= \frac{E_z(y)}{2} \exp j(\omega_e t - k_e y) + \text{c.c.} \quad \text{(input optical wave)} \\
\hat{E}_x(y,t) &= \frac{E_x(y)}{2} \exp j(\omega_o t - k_o y) + \text{c.c.} \quad \text{(output optical wave)} \qquad (1) \\
\hat{S}_6(y,t) &= \frac{S_6(y)}{2} \exp j(\omega_a t - k_a y) + \text{c.c.} \quad \text{(acoustic shear wave)}
\end{aligned}$$

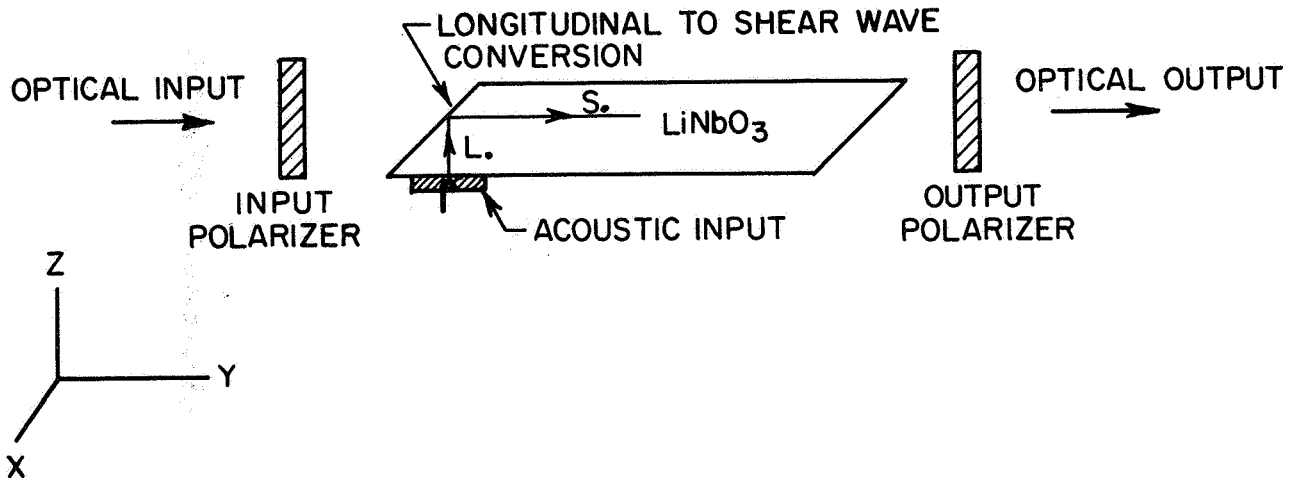

FIG. 1--$LiNbO_3$ acousto-optic filter. Longitudinal wave (L), shear wave (S).

The quantities ω_e , ω_0 , ω_a , and k_e , k_0 , k_a are the angular frequencies and $\bar{k}$ vectors of the input optical wave, output optical wave, and acoustic wave, respectively. The acoustic wave mixes with the input optical signal to produce forcing optical polarization waves at frequencies $\omega_e + \omega_a$, and $\omega_e - \omega_a$. These forcing waves propagate with $\bar{k}$ vectors of magnitude $k_e + k_a$ and $k_e - k_a$, respectively. Only if the $\bar{k}$ vector of this forcing wave is equal or nearly equal to that of the freely propagating electromagnetic wave, will a cumulative interaction over many wavelengths take place. In $LiNbO_3$ the ordinary refractive index is greater than the extraordinary index, which for forward propagating waves requires phase matching such that $k_e + k_a = k_0$, and which in turn results in the frequency of the ordinary wave (the output frequency in our example) being greater than that of the extraordinary wave by ω_a .

The interaction between the acoustic and optical waves takes place as a result of the photoelastic effect. This effect is described as a perturbation of the elements of the impermeability tensor b_{ij} such that $\Delta b_{ij} = p_{ijkl} S_{kl}$ where p_{ijkl} are the components of the photoelastic tensor and S_{kl} is the propagating strain wave. This perturbation of the impermeability tensor is equivalent to the creation of a driving polarization, which for our example may be shown to be given by

$$\hat{P}_x = - e_0 n_0^2 n_e^2 p_{41} \hat{S}_6 \hat{E}_z$$

$$\hat{P}_z = - e_0 n_0^2 n_e^2 p_{41} \hat{S}_6 \hat{E}_x \qquad (2)$$

where e_0 is the dielectric constant of free space and n_0 and n_e are the refractive indices for the ordinary and extraordinary waves respectively. If we substitute Eqs. (1) and (2) into the one-dimensional driven wave equation for lossless media, i.e.,

$$\frac{\partial^2 \hat{E}}{\partial y^2} - \frac{1}{c^2}\frac{\partial^2 \hat{E}}{\partial t^2} = \mu_0 \frac{\partial^2 \hat{P}}{\partial t^2} \tag{3}$$

and make use of the fact that $E_z(y)$ and $E_x(y)$ are slowly varying functions of y, then the following coupled complex equations may be obtained

$$\begin{aligned} \frac{dE_x}{dy} &= j \frac{n_0 n_e^2 p_{41} \omega_0}{4c} S_6 E_z \exp j\Delta k y \\ \frac{dE_z}{dy} &= j \frac{n_e n_0^2 p_{41} \omega_e}{4c} S_6^* E_x \exp - j\Delta k y \end{aligned} \tag{4}$$

where we have defined a $\bar{k}$ vector mismatch $\Delta k = k_0 - k_e - k_a$. In these equations the acoustic wave is assumed to propagate losslessly and thus the acoustic strain S_6 is assumed to be independent of position in the crystal.

Equations (4) are now solved subject to the boundary condition that $E_x = 0$ and $E_z = E_z(0)$ at $y = 0$. The ratio of the output power at $y = L$, $P_x(L)$, to the input power at $y = 0$, $P_z(0)$ is found to be given by

$$\frac{P_x(L)}{P_z(0)} = \left(\frac{\omega_0}{\omega_e}\right) \Gamma^2 L^2 \frac{\sin^2 \left(\Gamma^2 + \frac{\Delta k^2}{4}\right)^{1/2} L}{\left(\Gamma^2 + \frac{\Delta k^2}{4}\right) L^2} \tag{5}$$

where

$$\Gamma^2 = \frac{n_0^3 n_e^3 p_{41}^2 \omega_0 \omega_e}{16\, c^2} |S_6|^2$$

We note that the frequency of the transmitted optical signal differs from that of the input signal by the acoustic frequency ω_a . There is also an insignificant Manley-Rowe type power gain of magnitude ω_0/ω_e , which we will neglect in the following.

III. TRANSMISSION, TUNING RATE, BANDWIDTH, AND APERTURE

From Eq. (5) it is clear that the maximum transmission of the filter will be attained when the input optical frequency is such that the momentum mismatch $\Delta k = 0$. For this condition we have

$$\frac{P_x(L)}{P_z(0)} = \sin^2 \Gamma L \qquad (6)$$

and thus for theoretical 100% peak filter transmission we require that $\Gamma L = \pi/2$. Expressing $|S_6|^2$ in terms of the acoustic power density P_A/A , we obtain

$$\Gamma^2 = \frac{n_0^3 n_e^3 p_{41}^2 \pi^2}{2 \lambda_0^2} \frac{1}{\rho V^3} \frac{P_A}{A} \qquad (7)$$

where λ_0 is the optical wavelength, ρ is the density of the medium, and V is the acoustic velocity.

For a five cm long crystal of $LiNbO_3$ at a central transmission frequency of $\lambda_0 = 5000$ Å , we have $p_{41} = .155$,[3] $n_0 = 2.3$, $n_e = 2.2$, $\rho = 4.64$ gm/cm^3 , $V = 4.0 \times 10^5$ cm/sec ; and find that we therefore

require an acoustic power density of 14 mw per mm^2 of filter aperture for 100% peak transmission.

With the acoustic power adjusted to provide peak transmission at the center frequency ($\Gamma L = \pi/2$), the frequency response of the filter is determined by the variation of Δk as the optical frequency is changed. We let

$$\Delta k = \left(\frac{\partial k_o}{\partial y} - \frac{\partial k_e}{\partial y}\right)\Delta y \equiv b\Delta y \tag{8}$$

where Δy is the change in wave numbers of the optical frequency from the center frequency of the filter. From Eq. (5), the optical frequency response function of the filter $H(f)$ may then be written

$$H(f) = \pi^2 \frac{\sin^2 \frac{1}{2}(\pi^2 + b^2L^2\Delta y^2)^{1/2}}{\pi^2 + b^2L^2\Delta y^2} \tag{9}$$

Figure 2 shows the transmission $H(f)$ plotted versus the normalized frequency variable $bL\Delta y$. It is seen that the half-power transmission points of the primary lobe of the filter occur when $bL\Delta y \cong \pm 2.5$. For $LiNbO_3$ the constant b may be obtained by differentiation of the Sellmeier equations of Hobden and Warner.[4] The result of this differentiation is given in Fig. 3, as a function of the optical wavelength at a temperature of 200°C. This temperature was chosen since $LiNbO_3$ exhibits optical damage at temperatures lower than about 160°C.[5] It is seen that b is somewhat larger than the value $2\pi(n_o - n_e)$, which it would have in the absence of optical dispersion. The quantity $2\pi(n_o - n_e)$ is also shown in Fig. 3. For a 5 cm long crystal of

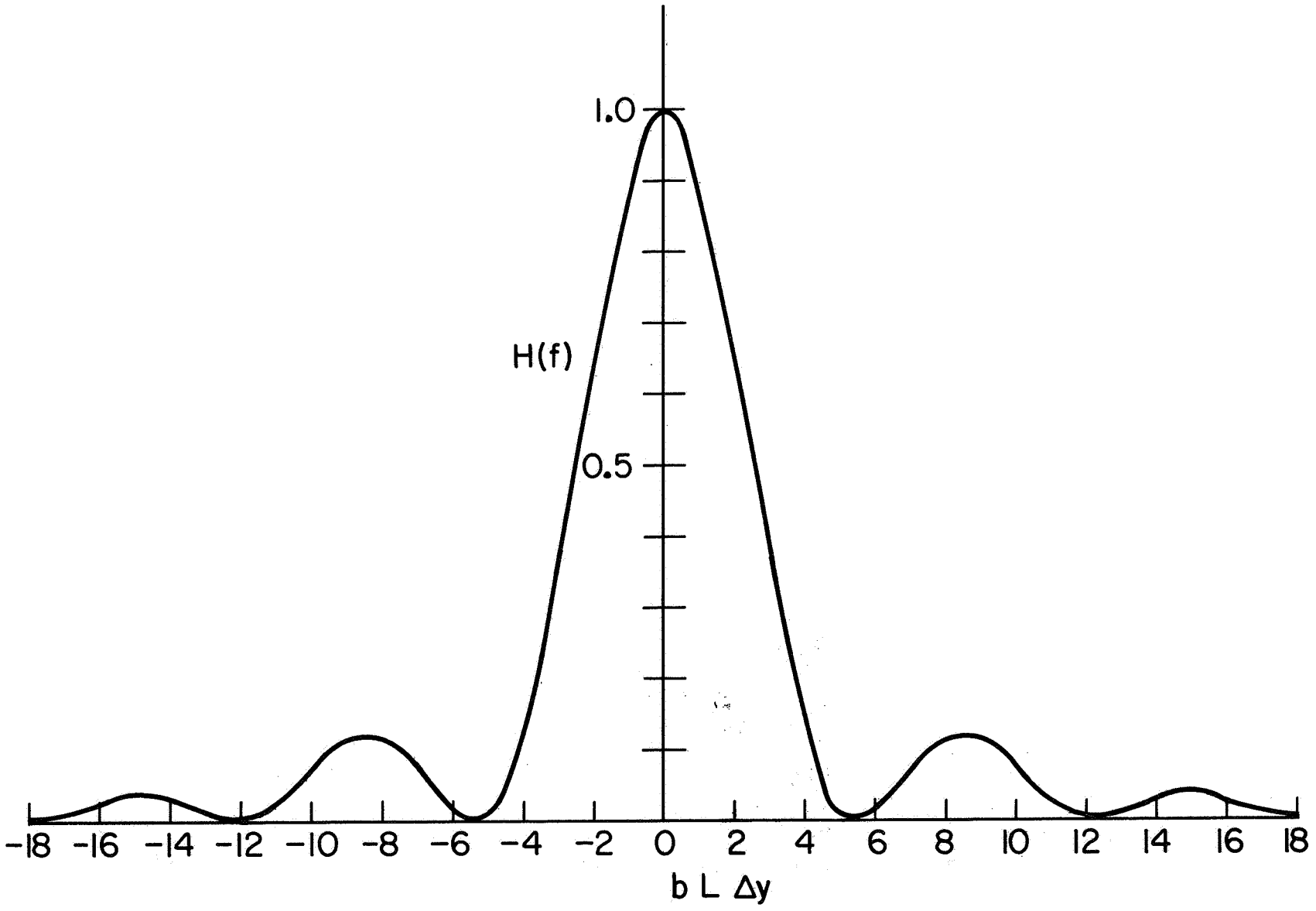

FIG. 2--Filter transmission vs normalized frequency.

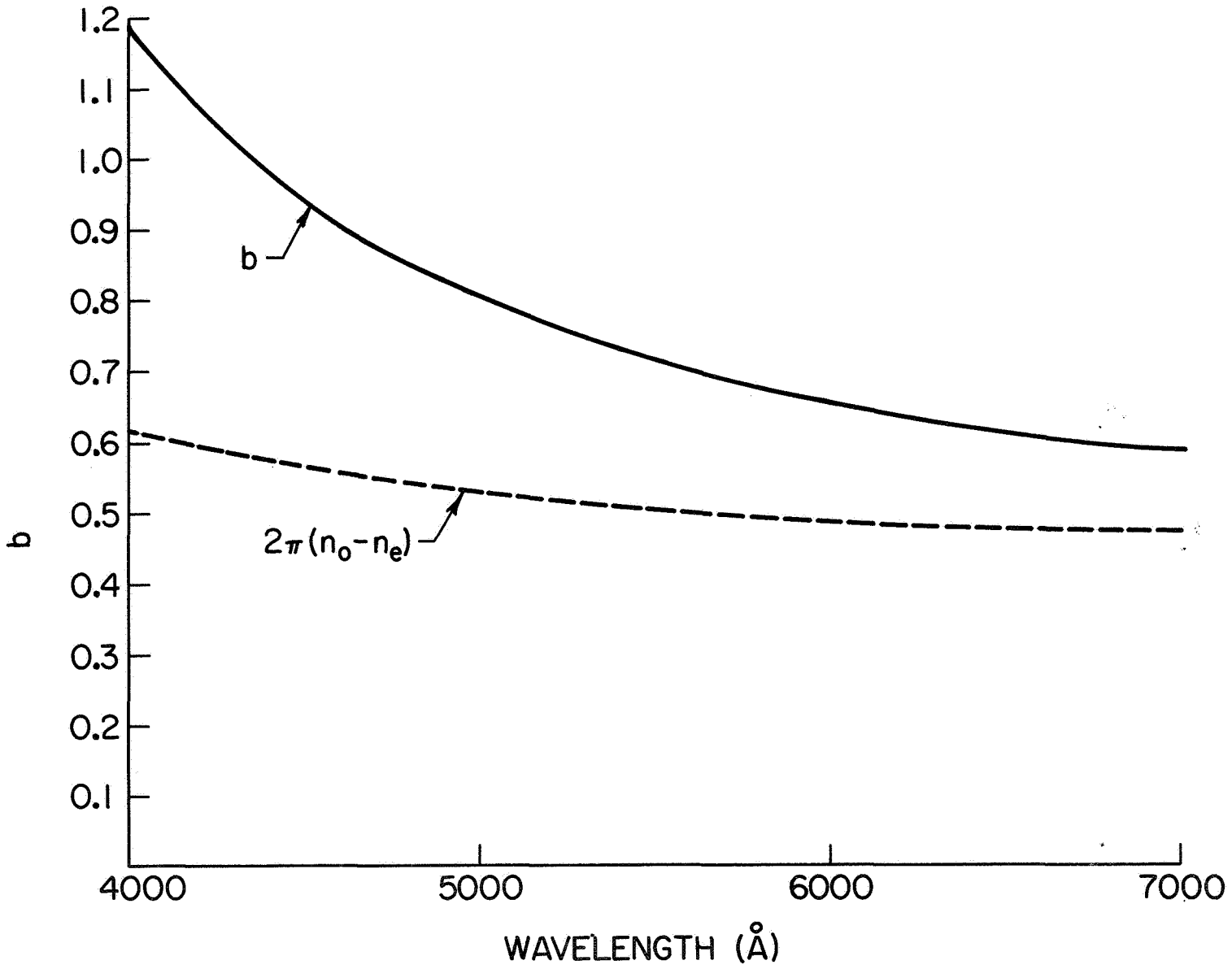

FIG. 3--b and $2\pi(n_o-n_e)$ vs λ .

$LiNbO_3$ at 5000 Å the total half-power bandwidth of the first lobe of the filter ($\tilde{=} 5/bL$) is about 1.25 cm^{-1} = .31 Å .

Electronic tuning of the filter may be accomplished by changing the frequency of the acoustic wave, and thereby changing the length of its $\bar{k}$ vector. The acoustic frequency which will yield peak transmission at an optical wavelength λ_0 is

$$f_a = \frac{V}{\lambda_0}(n_0 - n_e) \qquad (10)$$

where V is the acoustic velocity. For $LiNbO_3$ $V = 4 \times 10^5$ cm/sec and $n_0 - n_e$ may be obtained from Fig. 3. The necessary acoustic frequency for peak transmission at 5000 Å is 680 Mc, and the region from 7000 Å to 4000 Å can be tuned by changing the acoustic frequency from about 428 Mc to about 990 Mc . The rate of change of optical wave number per cycle change in the acoustic frequency is $\Delta y/\Delta f_a = 2\pi/bV$ where b is defined in Eq. (8) and plotted in Fig. 3. We see that the average tuning rate for $LiNbO_3$ is about 20 wave numbers per Mc change in the acoustic frequency. It should be noted that as the acoustic frequency is changed, that the acoustic power level should be varied inversely as the square of the acoustic frequency if 100% peak filter transmission is to be maintained [note Eqs. (6), (7), and (10)].

The optical angular aperture of the filter at the input frequency corresponding to peak collinear transmission is determined by $\bar{k}$ vector mismatch. The half power, half angle aperture occurs when $\Delta kL \tilde{=} \pi$.

For nearly collinear propagation we obtain from Fig. 4

$$\begin{aligned} \Delta k &= k_0 \cos\varphi - k_e \cos\psi - k_a \\ &\cong k_0 - k_e - k_a + \left(k_e - \frac{k_e^2}{k_0}\right)\frac{\psi^2}{2} \\ &\cong \frac{\pi}{\lambda}\Delta n\, \psi^2 \end{aligned} \tag{11}$$

The half-angle aperture taken inside the crystal is then about $\psi = \sqrt{\lambda/L\Delta n}$. This is magnified by refraction at the input of the crystal to yield a total aperture of about $2n_e\sqrt{\lambda/L\Delta n}$. For a 5 cm crystal of $LiNbO_3$ at $\lambda = 5000$ Å , this yields a half-power aperture external to the crystal of approximately .02 radians or 1.15°.

IV. DISCUSSION

Probably the most severe limitation of the proposed filter is the difficulty of obtaining large apertures. Since we require 14 mw of propagating acoustic power per mm^2 of crystal aperture, a 1 cm square aperture would require an acoustic power of 1.4 watts. Broadband r-f to acoustic transducers can now be constructed with about 10 dB conversion loss, thus requiring an r-f power of 14 watts. Also, at frequencies in the 400 to 1000 Mc range, the construction of transducers having one cm^2 of area is somewhat ahead of the present state of the art.

It should also be noted that the present analysis has neglected the acoustic attenuation which occurs as the acoustic wave propagates down the crystal. At room temperature this attenuation should be about 3 dB at 1000 Mc,[6] and vary approximately as the square of the acoustic frequency. Its effect will be to effectively shorten the crystal and thus

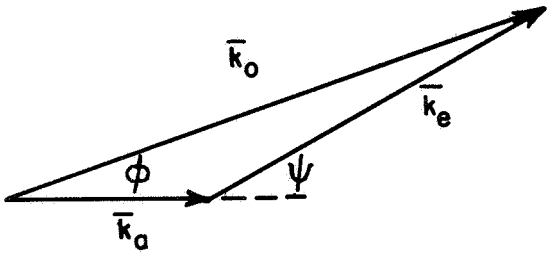

FIG. 4--$\bar{k}$ vector matching for nearly collinear propagation (not to scale).

to lead to somewhat larger bandwidths and necessitate somewhat higher acoustic drive powers.

The particular choice of $LiNbO_3$ and the filter configuration of Fig. 1 is only one of a number of possible crystals and configurations which could be employed. The advantage of this configuration is that it allows the acoustic wave to be brought in at right angles to the light, and thus does not require the light to pass through an acoustic transducer. A disadvantage is that for shear wave propagation down the y-axis there is approximately a 7° walk-off between the direction of the acoustic power flow and the acoustic $\bar{k}$ vector. This requires that the filter aperture be at least one part in ten of the crystal length. There are, however, other crystal orientations which allow diffraction into the orthogonal polarization and do not exhibit this walk-off. For example, collinear propagation of a longitudinal acoustic wave and the optical signal down the x-axis of a $LiNbO_3$ crystal accomplishes the desired result.[1]

Two other materials which may be useful for this type of filter are sapphire and quartz,[1] which have the same photoelastic tensor as does $LiNbO_3$. The birefringence of both of these materials is about 1/10 that of $LiNbO_3$. As a result the necessary acoustic frequencies would be centered about 70 Mc instead of 700 Mc as in the $LiNbO_3$ filter. Both the tuning rate and also the bandwidth of these filters (for the same crystal length) would be about ten times as large as that of the $LiNbO_3$ filter. The angular aperture would be about three times as large as that of a $LiNbO_3$ filter of the same length. As a result of the lower refractive indices of these crystals, about ten to twenty

times as much acoustic power would probably be required to obtain the theoretical 100% peak transmission. However, this might be off-set by using longer crystals.

It is planned that the construction of an experimental model of an acousto-optic filter will begin shortly in our laboratory.

ACKNOWLEDGEMENT

The authors gratefully acknowledge many helpful discussions with C. F. Quate.

REFERENCES

1. R. W. Dixon, "Acoustic Diffraction of Light in Anisotropic Media," IEEE J. Quant. Electr. QE-3, 85-93 (February 1967).
2. E. G. H. Lean and H. J. Shaw, "Efficient Microwave Shear-Wave Generation by Mode Conversion," Appl. Phys. Letters 9, 372-374 (November 1966).
3. R. W. Dixon, "The Photoelastic Properties of Selected Materials and their Relevance for Applications to Acoustic Light Modulation and Scanners," J. Appl. Phys. (to be published).
4. M. V. Hobden and J. Warner, "The Temperature Dependence of the Refractive Indices of Pure Lithium Niobate," Phys. Rev. Letters 22, 243-244 (August 1966).
5. A. Ashkin, G. D. Boyd, J. M. Dziedzic, R. G. Smith, A. A. Ballman, J. J. Levinstein, and K. Nassau, "Optically Induced Refractive Index Inhomogeneities in $LiNbO_3$ and $LiTaO_3$," Appl. Phys. Letters 9, 72 (July 1966).
6. C. P. Wen and R. F. Mayo, "Acoustic Attenuation of a Single-Domain Lithium Niobate Crystal at Microwave Frequencies," Appl. Phys. Letters 9, 135 (August 1966).